Impacts of permafrost degradation on an arctic polygonal mire (Alaska, 60º): A geochemical and geomorphological approach

---

Final Bachelor's Project

Double Degree in Environmental Sciences and Geology

Faculty of Sciences

June 2020

Irregular low centered ice wedge polygons North Slope, Alaska. From Ina Timling.

Author: Gabriel Miret Minard

Supervisors: Olga Margalef Marrasé

Oriol Grau Fernàndez

En record teu, Guillem

Index

Acknowledgements....4
Abstract....5
1 Introduction....6
1.1 Objectives....7
1.2 Study site....7
2 Methodology....9
2.1 Field work....9
2.2 Laboratory work....10
2.2.1 Densities....10
2.2.2 ICP-MS....10
2.2.3 IRMS....10
2.2.4 pH measurements....10
2.3 Geomorphological mapping....10
2.4 Data analysis....11
3 Results....11
3.1 Geochemical analyses....11
3.1.1 Depth distribution....11
3.1.2 Features distribution....12
3.2 Geomorphological results....14
3.2.1 Carbon Stock estimation....14
4 Discussion....14
4.1 Geochemical approach....14
4.1.1 Depth distribution....14
4.1.2 Microtopographic effects....16
4.2 Geomorphological approach....17
5 Conclusions....18
6 References....19
Annexes....22
Annex 1: Field scenes of the studied features....22
Annex 1: Landsat 8 scene of the studied area with b.c. 6-5-2....23
Annex 2: Cartography of Northern Alaska....24

Acknowledgements

Having finished to write this project, I would not feel at ease without acknowledging everyone that has helped me during the time I have worked on it, especially after this strange semester we have lived.

Firs of all, I sincerely want to thank my supervisors Olga and Oriol. Even though at first I was rather lost and unsure about which direction to take, you always helped and encouraged me to do a good job and get the best out of myself.

I also thank my fellow double degree friends. It has been five long years, but they have flown by between classes and field trips. I would like to particularly thank you all for this last semester. Even from the distance, we helped each other and, in the end, we made it. Without you, it would have been much harder to keep the rhythm without losing focus on this project.

Finally, I want to thank my family and close friends for their constant support. Especially to my parents which have had to cope with me these last three months and my two brothers, Joan and Roger, for their advises and reassuring me with their particular humor.

Abstract

Polygonal mires are characteristic of Arctic lowlands and store one third of the world's soil carbon. Under global warming, they are vulnerable to degradation, leading to changes in the landscape known as thermokarst and ultimately to the release of labile carbon; methane emission to the atmosphere and altering their ecosystems. This study describes the landscape of a thermokarst affected polygonal mire in the North Slope, Alaska through the mapping of thermokarst landforms; and examines the spatial interactions of active layer biogeochemistry across different microtopographic features in a thermokarst lake basin from the site. Significant differences were found with depth distribution and between the most extreme permafrost degrading and non-degrading features, demonstrating important multidimensional aspects of polygonal ground biogeochemistry and the impacts of thawing of the ice ground. The mapped thermokarst landforms cover suggests that thermokarst lake forming might be related to the terrain slope condition. The results of this study provide more information for understanding how polygonal ground systems function, and how they may respond to future change.

Les torberes poligonals són característiques de les planes baixes de l'Àrtic i emmagatzemen un terç de l'estoc de carboni del sòl mundial. Amb l'escalfament global, els canvis del paisatge coneguts com a termokarst provoquen la degradació de les torberes i, en última instància, l'alliberació de carboni làbil; emissió de metà a l'atmosfera i l'alteració dels seus ecosistemes. Aquest estudi descriu el paisatge afectat per termokarst d'una mollera poligonal del North Slope d'Alaska fent una cartografia de les estructures de termokarst; i examina les interaccions espacials de la bioquímica de la capa activa a través de les diferents estructures microtopogràfiques d'una de les conques d'un llac termokàrstic drenat. S'han trobat diferències significatives en la distribució pel que fa a la profunditat dels elements analitzats i entre les estructures que representen els extrems de degradació del permafrost, demostrant aspectes multidimensionals importants de la bioquímica i els impactes que té la fusió permafrost en aquests sòls. La cartografia suggereix que la formació de llacs termokàrstics pot estar estretament relacionada amb el pendent del terreny. Els resultats d'aquest estudi aporten informació per entendre com funcionen aquests sistemes i com poden respondre als canvis en el futur.

Las turberas poligonales son características de las planas bajas del Ártico y almacenan un tercio del carbono del suelo mundial. Con el calentamiento global, los cambios del paisaje conocidos como termokarst provocan la degradación de las turberas y, en última instancia, la liberación del carbono lábil; emisiones de metano a la atmósfera y la alteración de sus ecosistemas. Este estudio describe un paisaje afectado por termokarst de una mollera poligonal del North Slope en Alaska, con la cartografía de las estructuras típicas de termokarst; y examina las interacciones espaciales de la bioquímica de la capa activa a través de sus diferentes estructuras microtopográficas que se forman en una de las cuencas de un lago termokárstico drenado. Se han encontrado diferencias significativas en la distribución en profundidad de los elementos analizados y entre las estructuras que representan los extremos de degradación del permafrost, demostrando así aspectos multidimensionales importantes de la bioquímica y los impactos que tiene la fusión del permafrost de estos suelos poligonales. La cartografía realizada sugiere que la formación de lagos termokársticos puede estar estrechamente relacionada con el pendiente del terreno. Los resultados del estudio aportan información útil para entender cómo funcionan estos sistemas y como pueden responder a futuros cambios.

1 Introduction

Peatlands are areas with the water table at or near the surface, where peat has accumulated and formed a layer of at least 30-40 cm thick. The storage of this amount of organic matter is only possible when plant-matter accumulation rates exceeds oxidation and decomposition rates by microorganisms. This happens because there is an oxidized zone in the upper active peat layer with a high hydraulic conductivity and fluctuating water table, and a more reduced inert and permanently saturated lower layer where peat material is no longer subject to significant decomposition (Ivanov, 1948).

Peatlands are found to be of utmost importance, as they have a critical role in carbon storage and climate change mitigation. Even though peatlands only cover approximately 3% of global land area, they store one third of the world's soil carbon (Parish et al., 2008). Most of this stock is stored in the northern circumpolar region, mostly in frozen peatlands (Hugelius et al., 2013). Large peatland/mire areas exist within the permafrost zones of Canada, Denmark/Greenland, Finland, Norway, Russia, Sweden and the United States, where the ground remains frozen at sub-zero temperatures for at least two consecutive years (Brown, 1960).

High altitude mires are vulnerable to degradation due to the loss of permafrost under a warming climate (Hugelius et al., 2014; Zhang et al., 2008). This could lead to the release of labile carbon, enhancing methane production and emission to the atmosphere (Walter et al., 2008). This issue is thus aggravated by global warming, especially in the Arctic region (60-90ºN) where is amplified (SWIPA, 2017).

Thaw of the underlying permafrost in these regions leads to distinctive depressions in the landscape, known as thermokarst. Typical thermokarst landforms include thermokarst lakes, sinkholes, pits, and troughs in polygonal terrain (Jorgenson et.al., 2008). Polygonal patterned ground is defined by a network of troughs and rims, pushed by the formation of ice wedges, ice veins that have grown underground by thermal crack and contraction. These create different reliefs, with depressed areas waterlogged where peat can grow and pile up (Ballantyne, C. K., 2018). However, water accumulating enhances heat gain and permafrost degradation in a positive feedback, leading to thermokarst features and, if not interrupted, finally subsidizing, and converting small bodies of water into lakes. The spread of these lakes, on the other hand, could also increase the connectivity of drainage networks, supporting lake drainage, which leaves an enclosed depression or *drained thermokarst lake basin* (DTLB) underlain by a talik which is progressively diminished in size by permafrost aggradation. In DTLBs is where preferential accumulation of peat occurs and polygonal mires are formed, re-establishing permafrost and peat accumulation and closing the thermokarst cycle (Jones et. al., 2012). Jorgenson et al. summarized these processes in a conceptual model (Fig. 1). However, ice volume, changes in reliefs and climate disturbances can affect thermokarst processes, involving other pathways for ice wedge dynamics (the cycle is not regular). These contrasting processes illustrate the uncertainties associated with predicting how permafrost thaw will alter the fate of the vast amount of stored carbon (Schuur et al., 2009). These uncertainties are propagated from the variability of many parameters and

underlying processes. These include, not only the complexity of geomorphological and hydrological properties of the tundra soils and its dynamics under a warming climate, but also our limited knowledge of the physicochemical and microbiological parameters of the permafrost soils, their effects on carbon degradation, and responses to future climate change (Jorgenson et. al., 2015).

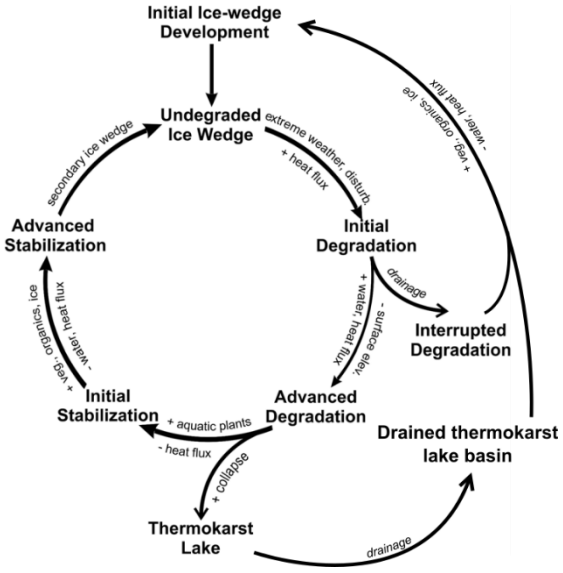

Fig. 1. Conceptual model of cyclic ice wedge degradation and stabilization. Main stages are shown in bold, while biophysical factors affecting transitions are shown along arrows. Positive feedbacks with increasing heat flux are on the right, while negative feedbacks with decreasing heat flux are on the left. Modified from Jorgenson et al., 2015.

1.1 Objectives

The aim of this study is to provide more information about the thaw of permafrost in arctic mires and its effects on a microtopographic level.

To achieve this, the following specific objectives were planned:

- Mapping and characterizing the geomorphological features of a thermokarst landscape in a floodplain peatland of the Northern Slope of Alaska

- Interpret the depth distribution of analytes and compare the physicochemical differences and dynamics of the different stages and landforms of the polygonal ground pattern through the sampling of one of the partially drained thermokarst lake basins of the mapped area.

- Estimate the stored carbon of the basin and compare it with previous observations of similar areas.

1.2 Study site

This study focuses on a 27.500 ha area (Fig. 2) located on a lowland plain including the Sagavanirktok river at the Foothill of the North Slope, Alaska (69°32'16.30"N 148°40'4.78"O). The studied area was chosen as it is within and represents the Foothills zone of the North Slope, at the limit with the Brooks Range, where few studies exist regarding permafrost thawing and its physicochemical impacts. The geochemical analysis focuses on a smaller area, a DTLB partially filled with water (called *Broken Tooth*) chosen because it was fully covered by peat and showed all the different states (and associated features of a polygonal mire) defined in Fig. 1.

The upland geology of the study area is comprised basically by organic ice-rich silt (loess) and some fluvial coarse sediments deposited during the late Pleistocene (Wilson, F. H. et al., 2015). The fluvial sediments come mostly from the erosion of the Brook Range deposits, uplifted due to the development of an extensional rift in the north (Beaufort Sea) during the Early Jurassic and Early Cretaceous 190-120 million YBP (years before present). Brook Ranges' materials comprise all geological periods from the Paleozoic Era (even a little

bit of Proterozoic) to the Quaternary Period. However, to the south from the studied area these materials are more characterized by limestone and carbonate deposits from a continental shelf and abyssal plain (Carboniferous), which when uplifted they were metamorphosed to marble; and loess silt (moraines) sediments from glaciers (Pliocene to Holocene). In some areas Cretaceous igneous materials (granites) also emerge (Fig. 3). The studied area remained unglaciated during the Last Glacial Maximum (LGM) (ca. 21,000 YBP (Kaufmanand Hopkins, 1986), differentiating this area within just a few kilometers south where deposits were affected by glaciers.

The climate of this region is typical of the northern arctic zones, with a mean annual air temperature of -5,5ºC, mean annual soil temperature of 0,36 ºC (0 cm) and -0,27 ºC (100 cm) and a mean annual precipitation of 552,2 for the period 2018-2019. (Toolik Field Station, http://toolik.alaska.edu/edc/abiotic_monitoring/data_query.php). Permafrost reaches depths of more than 300 m (Jorgenson et al., 2008), with total volumetric ice contents ranging from 40 to 90% (Kanevskiy et al., 2013; Jorgenson et al., 2008).

The North Slope is characterized by thousands of thermokarst lakes and DTLBs which cover up to 20,4% and 25,7% of the area respectively (Frohn et al, 2005).

The general geomorphology of the Foothills is characterized by floodplains with abundant thermokarst lakes and DTLBs that have subsided and contain numerous small meandering streams and beaded streams. Thermokarst lakes usually form by subsidizing of thermokarst affected terrain, but to initiate thermokarst there needs to be a change in the heat balance at the surface. Thus, in this area has been noted in previous observations (Pestryakova et al., 2012; Jorenson and Shur, 2007) that original shallow oxbow lakes in abandoned river meanders might evolve as thermokarst lakes, as they would provide a heat gain needed to start the thermokarst cycle. Beaded streams are channels with regularly spaced deep and elliptical pools connected by narrow runs and are a common form of many streams that drain Arctic permafrost foothills and lowlands. They are thought to be a common arctic thermokarst landform and occur mainly in association with ice-wedge networks of polygonized tundra (Arp, C. D. et al, 2015).

The studied polygonal peatland is classified as a mineratrophic mire, as it is reliant on groundwater for water and nutrient supply (although it also has precipitation and surficial flooding as secondary sources). It is differentiated from ombrotrophic peatlands, which are dependent on precipitation for water and nutrient supply and are more acidic (ph values of 3-6) than mineratrophic mires (ph 6-8) (Martini et al., 2006).

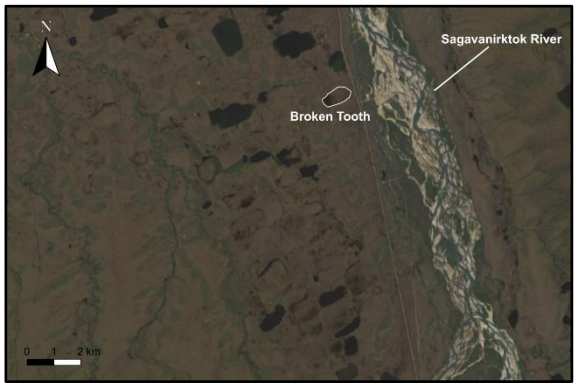

Fig. 2. Studied area from a Landsat 08 scene. The Sagavanirktok river and the Broken Tooth DTLB are marked.

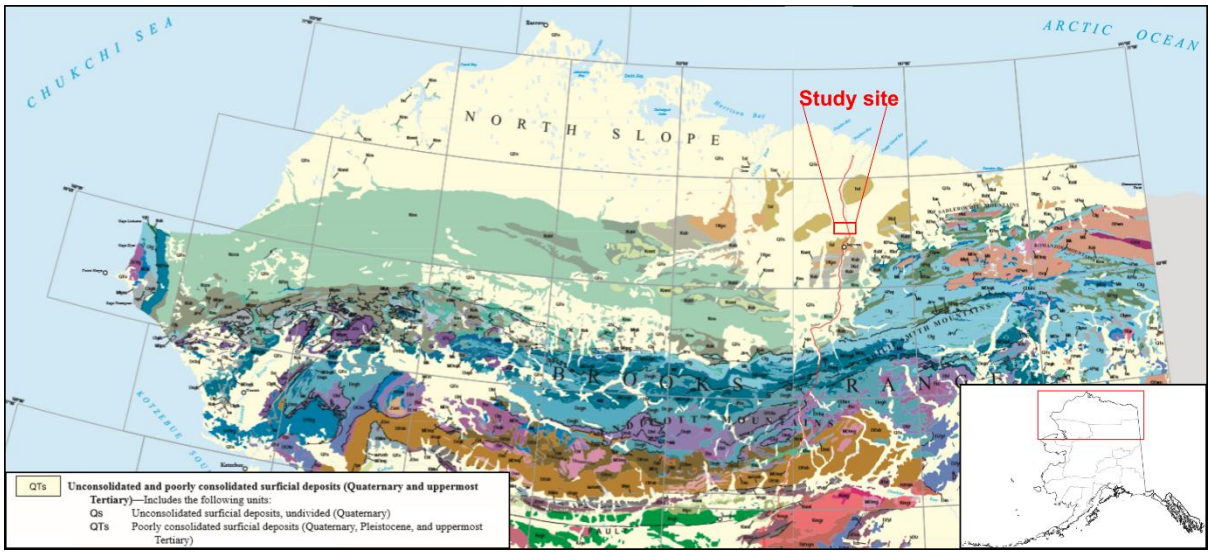

Fig. 3. Geologic map of the northern area of Alaska, with the Brooks Range and North Slope comprised in it. The study site is marked in red in the geologic map. Modified from Wilson, F. H. et al, 2015.

2 Methodology

2.1 Field work

Soil sampling in the *Broken Tooth* drained basin (Fig. 4) was done by Dr. Margalef and Dr. Grau from CREAF, and Dr. Joosten from the University of Greifswald in August 2019.

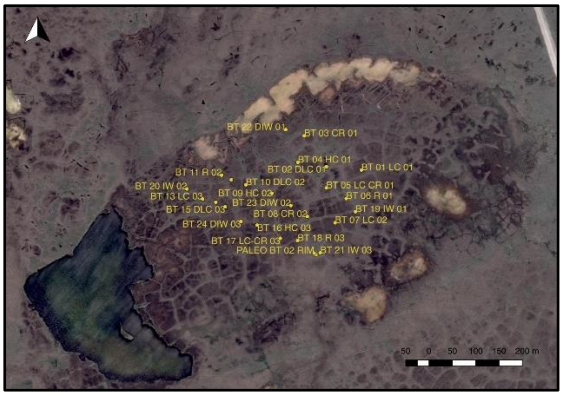

Fig. 4. Broken tooth, DTLB partially filled where the samples were taken (69º34'11,42"N, 148º38'18,74"W). From Margalef, 2019.

Five different features within the polygonal mire were chosen to analyze the effect of permafrost thawing on soil geochemistry. These include features in the initial state of a polygonal mire, represented by low center polygons (LCs) and rims (Rs). LCs can then develop into depressed low centers (DLCs) when thawing of the PF layer and deepening of the active layer are aggravated; or into high centers (HCs) in the opposite case, when waterflow drains towards the polygon edges enhancing the PF development towards the surface and the reduction of the active layer. When this happens, water promotes the thawing of the ice wedge, thereby subsidizing the area above it, and creating a collapsed rim (CR) (Fig. 5). Field scenes of this structures are included in Annex 1.

Three replicate cores were drilled for each feature. To avoid spatial aggregation the features sampled were randomly selected across the area (Fig. 4). For each core, four different samples were collected at different depths: upper and bottom part of the first 15 cm of the active layer (A1 and A2, respectively), bottom of the active layer, 40-70 cm (B) and at the permafrost layer (PF).

The frozen soil was extracted using a permafrost driller coupled to an auger motor (Fig 6).

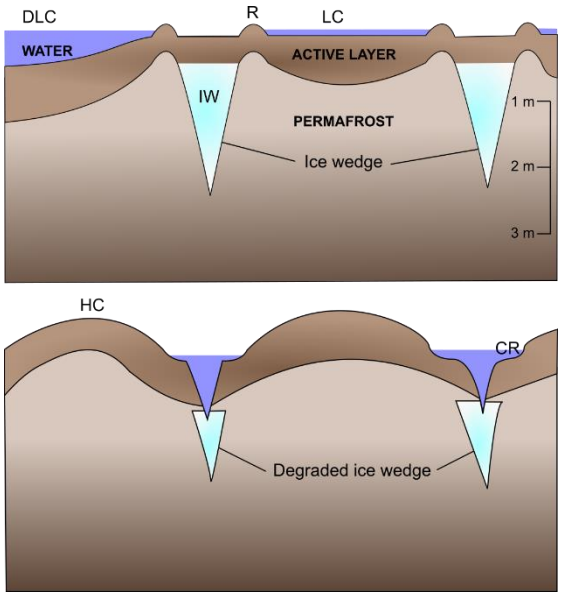

Fig. 5. Polygonal mire morphologies sampled in this study. The scale is approximated.

Fig. 6. Dr. Grau (left) and Dr. Joosten (right) taking a sample with the permafrost driller. Margalef and Grau (2020).

2.2 Laboratory work

The total of 89 samples were taken to the laboratory, where they were treated before proper analysis.

2.2.1 Densities

First, investigators Dr. Margalef and Dr. Grau from CREAF, laboratory supervisor Mr. Fernández and the author of this study calculated the densities of each sample by first weighing a portion of the sample with a precision weighing scale and then diving it in a water filled test tube to measure its volume.

2.2.2 ICP-MS

The elemental composition was determined by Inductively Coupled Mass Spectometry (ICP-MS). The author of this study personally dried and ground up with a ball mill (Retsch, 199 model MM400. Restch GmbH) a portion of each 89 of the samples in the chemistry laboratory in CREAF.

2.2.3 IRMS

The quantification of total C and N and their stable isotopes (13C and 15N) was done by UC Davis (California) using an Isotope Ratio Mass Spectrometer. The author of this study personally dried and ground up the samples and afterward laboratory supervisor Mr. Fernandez weighted them in tin capsules before sending them to California.

2.2.4 pH measurements

The method used to know the pH of the samples was through the dilution of a portion (2,5 g / 35 ml), centrifugation and finally measurement with a pH meter, which the author of this project did personally.

2.3 Geomorphological mapping

The map of major thermokarst landform units was created based on a resolution terrain-corrected Landsat 8 OLI/TIRS scene from 8 July 2019 (path 74, row 11) that the author of the study selected from the U.S. Geological Survey (https://earthexplorer.usgs.gov/). To manually map terrestrial landforms (bedded streams, thermokarst lakes and drained thermokarst lake basins) ArcMap from ArcGIS program was used, using the band combination 6-5-2 (6 – SWIR 1; 5 – near infrared; 2 – blue) as it differentiates greener healthy vegetation from red-brownish non-healthy vegetation (Annex 2). Visual interpretation and identification of drained lake basins

was aided by an image from Google Earth of the same site and year.

Thermokarst lakes were identified as bodies of water with minimum land cover of 20 ha. DTLBs were mapped with no differentiation even if they were only partially drained (with water bodies left).

For the area cover of the different mapped landforms, the geometric calculator from the same program was used.

2.4 Data analysis

A statistical analysis was carried by the author of the study from the data obtained in the different procedures to find significant patterns of the elements between these different thermokarst morphologies. A linear model as implemented in RStudio (v. 1.3.959; R Core Team, 2020) was used to assess the effect of morphology and depth on geochemical characteristics.

Following the same criteria used in previous studies (Michaelson et al., 1996), stock of carbon for the first meter from the surface was calculated. Calculations were as follows:

(1) Active layer for each replicate total C (g/cm^2): [(A1, A2 and B) Total C (%)/100 x (A1, A2 and B) Dry density (g/cm^3)]/3 x Active layer depth (cm)

(2) Permafrost layer for each replicate total C (g/cm^2): PF Total C(%)/100 x Dry density (g/cm^3) x (100 – active layer depth) (cm)

(3) Total C per land cover (kg/m^3) = (1) (kg/m^3) + (2) (kg/m^3)/number of replicates.

3 Results

3.1 Geochemical analyses

3.1.1 Depth distribution

The different elements and ratios analyzed in this study show existing differences in depth distribution. The concentration of C (carbon) decreases significantly (**) with soil depth between A1 and the B and PF layers (Fig. 7).

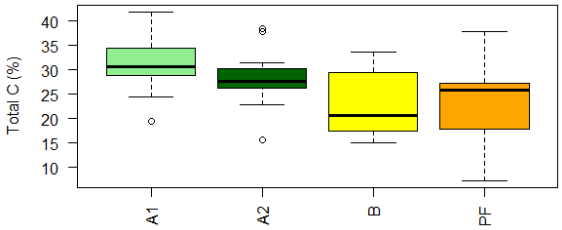

Fig. 7. Box plot for the depth distribution of total carbon (%) from all five different features.

Total N shows a similar pattern than total C, with a decrease of N compared to the surface, although less significant (*) in the PF layer (Fig. 8).

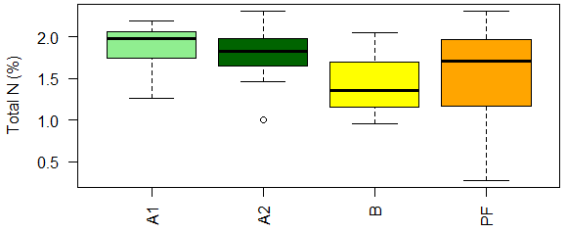

Fig. 8. Box plot for the depth distribution of total nitrogen (%).

Total P (phosphorus) and Fe (iron) measurements have an R^2 value of 0,22, which shows a significant correlation. They do not show a general significant difference in depth distribution (Fig. 9a).

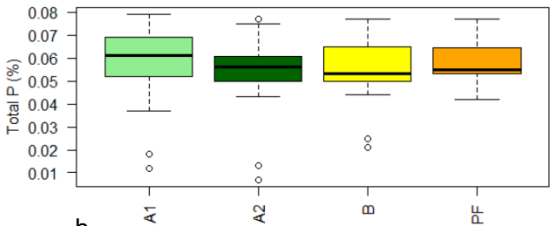

Fig. 9. Box plots for the depth distribution of total phosphorous.

The same happens for the general depth distribution of C/N/P ratios, where no significant differences have been found.

Aside from Ca and Fe, studied lithogenic elements (Na, Mg, Al, K and Ti) show similar behaviours regarding depth distribution (R^2 value between 0,7-0,9). As an example, Ti (titanium) has been chosen as a good proxy for detritical inputs due to its lithogenic origin and very low mobility. This is because Ti-bearing minerals have extremely low solubility and are not affected by redox changes. As seen in Fig. 10, there are very significant (***) lower values on the surface (A1) compared to B and PF depths.

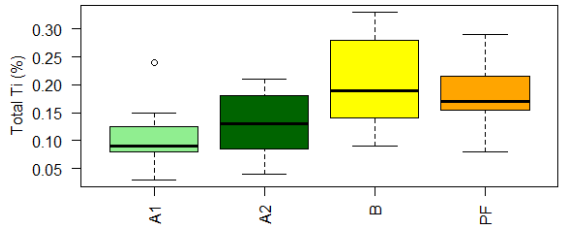

Fig. 10. Box plot for the depth distribution of total titanium (%).

Also, Ca does not either show any significant difference in depth distribution, although it seems to increase (Fig. 11).

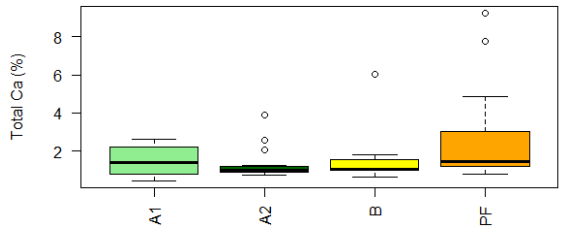

Fig. 11. Box plot for the depth distribution of total calcium (%).

3.1.2 Features distribution

Identifying significant differences between microtopographic landforms such as the studied ones in this study is important to understand soil dynamics and the effect of ground ice thawing. The following comparisons were done using only data from the upper part of the active layer (acrotelm) as it is where most runoff production and nutrient transfer occur, and thus where the effects of ice thaw and differences between features should be observed.

An initial state can be identified on polygonal mires where LCs and Rs are stablished (Fig. 5). In this case, although not significant, C/N ratio in rim shows higher values (Fig. 12a).

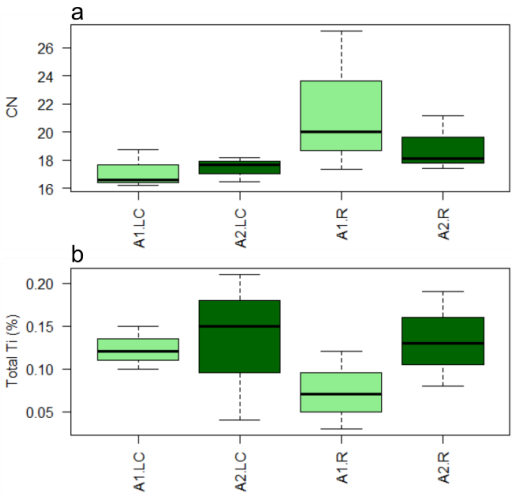

Fig. 12. Box plots of LC and R features in A layers for a) C:N ratio. b) Total titanium.

No other significant difference has been found, neither in C/N/P ratios or general lithogenic elements (Fig 12b).

However, there has been found a very significant difference in total Ca measurements, where in Rs the values are much higher than in LCs on the surface (Fig. 13a). This difference may explain the also significant (*) higher values of pH on the A layers in Rs (Fig. 13b).

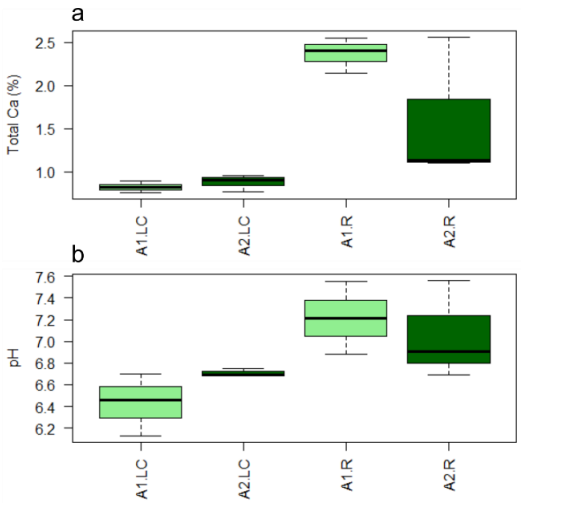

Fig. 13. Box plots of LC and R features in A layers for a) Total calcium. b) pH.

From the initial state, features can develop to more advanced thermokarst states, and here comparisons between these different states were used.

The first two compared features are Rs and CRs. The exact same differences from LCs and Rs are found between Rs and CRs, where there are no significant differences in most of the studied variables (Fig. 14a and b), but on the surface Ca values are significantly (**) higher in Rs (Fig 14c).

LCs can develop to DLCs when thawing of the PF layer and deepening of the active layer is aggravated, or to HCs in the opposite case, when waterflow migrates to the polygon edges enhancing the PF development towards the surface and the reduction of the active layer. In this study, between LCs and DLCs no differences have been found. However, significant (*) differences in N, P and N/C are shown between HCs/DLCs (Fig. 15) and marginally significant (.) for the same variables between HCs/LCs. In HCs N values are lower than DLCs and LCs, while C/N and P values are higher (Fig. 16).

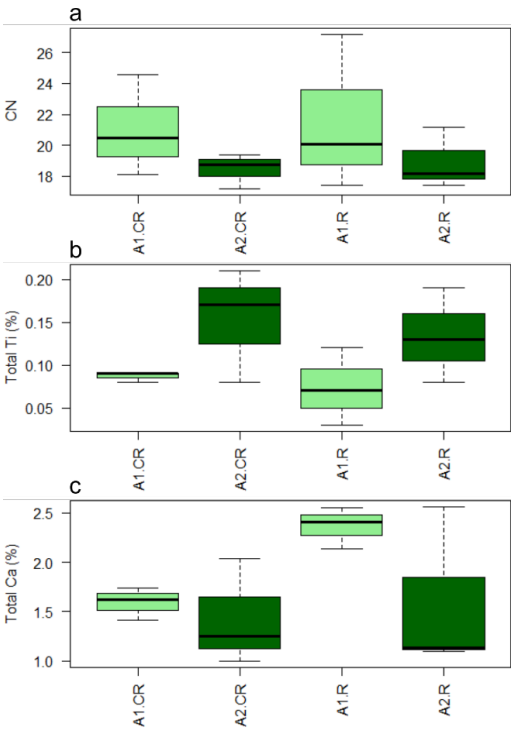

Fig. 14. Box plots of CRs and Rs features in A layers for a) C:N ratio. b) Total titanium. c). Total calcium.

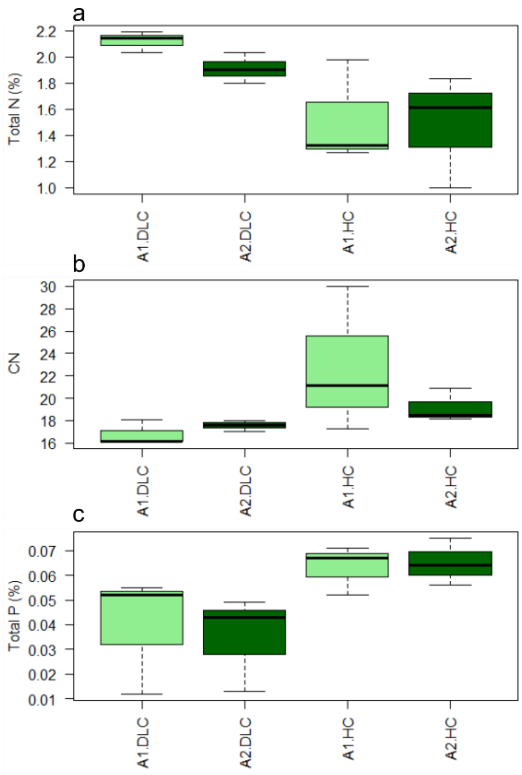

Fig. 15. Box plots of DLC and HC features on layers A for a) Total nitrogen. b) C:N ratio. c) Total phosphorus.

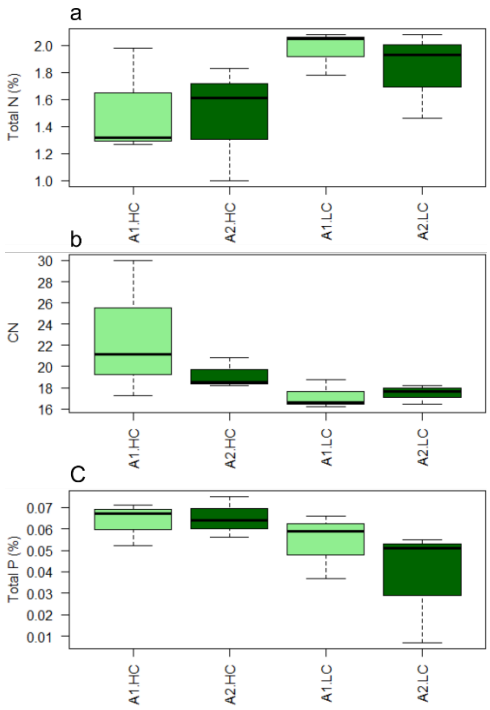

Fig. 16. Box plots of LC and HC features on layers A for a) Total nitrogen. b) C:N ratio. c) Total phosphorus.

3.2 Geomorphological results

The results obtained from the landform mapping of the studied area show that 15% of the area is affected by big thermokarst landforms, while 20% is basically covered by the Sagavanirktok river (19,7%) and then some streams (0,12%), leaving the 64% remaining terrain filled by plains with smaller features (such as less than 20 ha lakes and polygonal patterns). Drained thermokarst lake basins (DTLBs) occupy up to 12,5% of the studied area, while thermokarst lakes only cover the 2,5%. There is only one beaded stream which does not connect any DTLB or lake, and occupies 0,04% of the land and the rest of beaded streams which they do connect some of the DTLB with a land cover of 0,022% (Table 1).

In addition to being most numerous, DTLBs are the thermokarst landforms occupying the greatest mean surface area per individual feature, 54 ha (n = 64). Thermokarst-lakes have the second greatest mean surface area per individual feature, 41 ha (n = 17). Out of the 64 DTLBs, 23 are connected by smaller streams and only three from the 17 thermokarst lakes have no contact with at least one DTLB.

The mean size for the studied lakes is 43,22 ha and for the DTLBs 55,64 ha.

Half the studied area is covered by the river and land not affected by thermokarst. To be able to compare the results found in this study with previous studies, a representative focused area (FA) of 3444 ha inside the studied site was selected (Fig 17). In this area, 39,3% is affected from big thermokarst landforms. Out of this, 33,3% is from DTLBs and 5,8% from lakes. The remaining 0,2% is covered by beaded streams (Table 2).

Although normally thermokarst lakes have a preferent shape and direction, on the study site they show random shapes.

3.2.1 Carbon Stock estimation

Finally, the C stock by land cover calculated for the DTLBs soil is 77,25 kg/m^3, 53% accounting for the active layer and 47% for the permafrost layer.

4 Discussion

4.1 Geochemical approach

4.1.1 Depth distribution

The sharp decrease in total carbon and nitrogen concentrations with depth was expected. Even though at the surface level oxidation and decay processes are greater, the vegetation cover keeps providing organic matter. As this OM accumulates, the peat layer grows and deeper layers keep degrading at slower rates, resulting in additional carbon loss compared to the more recent surface peat (Kuhry and Vitt, 1996).

Table 1

Cover and number of landforms mapped in the studied area.

	Land cover (ha)	Cover (%)	Total number	Cover/ number
Beaded streams	17,03	0,06	11	11,37
Small streams	34,68	0,13	4	8,67
Thermokarst lakes	693,20	2,52	17	40,78
DTLB	3443,82	12,50	64	53,81
Sagavanirktok margin	2976,67	10,80	1	
Sagavanirktok bed	2430,43	8,82	1	
No big landforms area	17965,38	65,18		

Table 2

Cover and number of landforms mapped in the FA.

	Land cover (ha)	Cover (%)	Total number	Cover/ number
Beaded streams	5,87	0,10	9	0,65
Small streams	5,48	0,09	1	5,48
Thermokarst lakes	337,59	5,84	8	42,20
DTLB	1925,45	33,31	36	53,48
No big landforms area	3506,51	60,66		

The higher concentrations of lithogenic elements (Na, Mg, Al, K and Ti) with increasing depth, could be explained by the regional hydrology and geology. Some coarse sediments have been found on deeper samples (layer B and PF) interbedded within the peat record. These layers are related to old alluvial sediments brought by old floods. These sediments provide a supply of elements for these layers, especially in the PF layer, as the depositions happened mostly before the peat grew. The analysis of these coarse materials could provide information about which elements are more enriched by this source.

On the other hand, groundwater inflow above the permafrost layer plays a role on leaching of soluble nutrients (Na, Mg, K, Ca), but also as an input of them. Few studies have researched on these relationships and could explain an increase of these nutrients in the lower part of the active layer, which would justify the higher values found on the B layer.

Another explanation is suggested by Lacelle et al. (2007). They propose that increases in ion concentrations with depth should be typical in seasonally frozen soil, as solutes are concentrated in residual water at the bottom of the active layer during freeze back. They also suggested that the base of the active layer is dominated by chemical weathering which promotes enrichment. Both statements would add up to the high concentrations of solutes and low concentrations of elements hosted in minerals with low solubility (Ti and Al) found in this study in the B and PF layers.

All these hypotheses imply that the final elemental depth distribution is balanced by OM deposition and accumulation, rivers

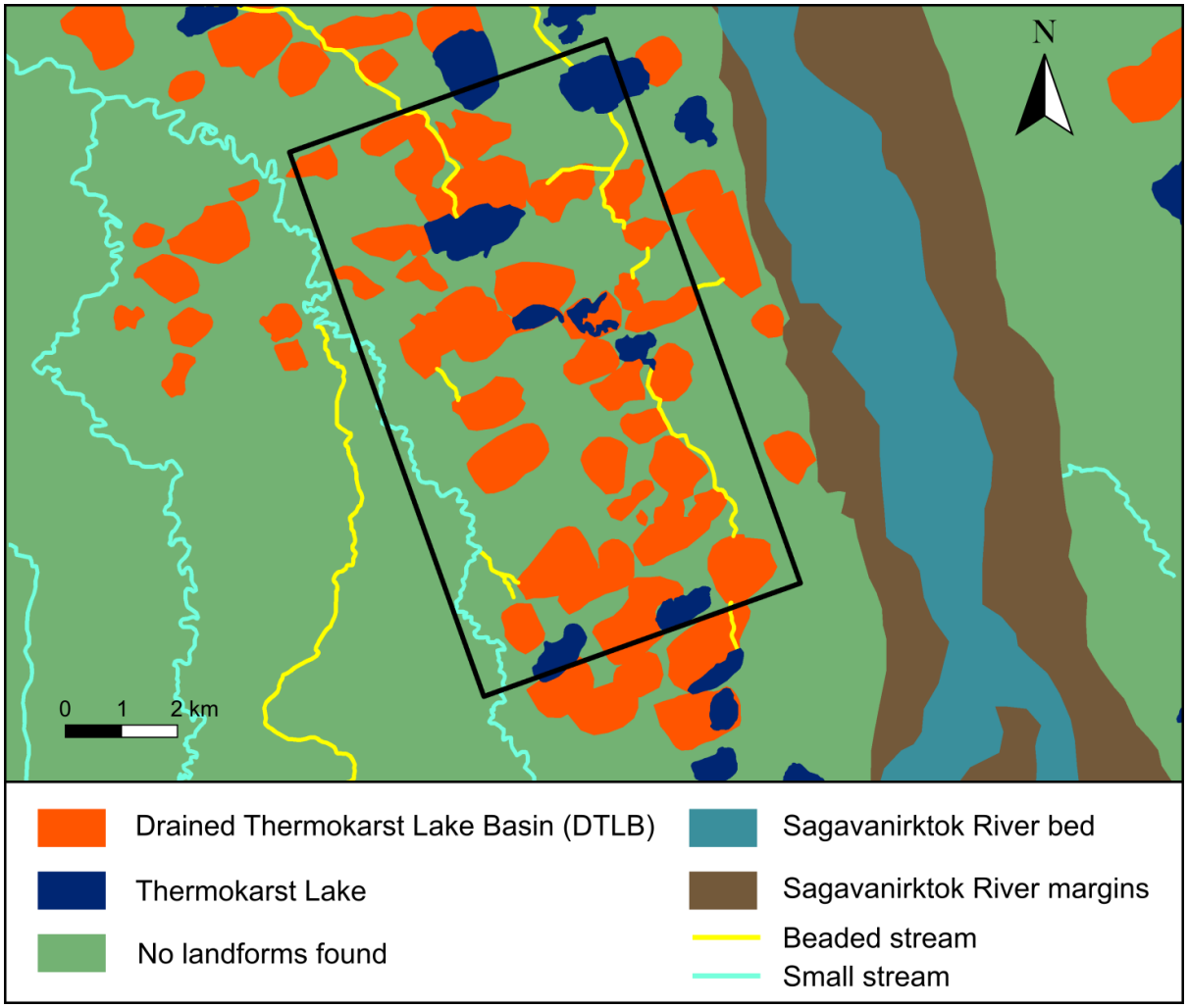

Fig. 17. Mapped study area with the FA defined inside the black rectangle.

detrital input, groundwater circulation and freeze-thaw seasonal processes. More focused studies about the controls on chemical variations with depth would be required to fully understand this balance.

4.1.2 Microtopographic effects

Comparisons between different features have shown significant differences basically between the most extreme degradation states of the microtopographic landforms (DLCs and HCs), although some others must be noted as well.

On the initial state, the higher C/N values found on Rs compared to LCs can be explained by the hydrological conditions of such features. The lower microtopographic position in the relief of LCs explains the permanent flood that accumulates organic and inorganic N. This explanation is consistent with previous studies of similar microtopographic features (Biasi et al., 2005; Giblin et al., 1991; Högberg, 2001; Kummerow et al., 1987). Furthermore, because the different vegetation that covers LCs shows a lower carbon concentration and higher C:N ratios, compared to the Rs' vegetation which is woodier.

A similar topography related process could explain differences in calcium between LCs and CRs with Rs. As the water table reaches the surface, LCs and CRs are waterlogged, which as stated before maintains a reduced environment, hampering organic matter oxidation and decay. However, higher relief in Rs makes them harder to be flooded,

creating more oxidized conditions and thus Ca being fixated to organic compounds and accumulating on the surface layers. This process has been observed in previous studies, where in more decomposed peats certain elements such as Ca were enriched (Martinez Cortizas et al., 2007; Biester et al., 2012). The same explanation can be applied for HCs, although no significant difference has been found. Furthermore, the high concentration of Ca translates to the higher pH values found on the surface of Rs and HCs.

Regarding the comparison between extreme degradation states, differences in organic compounds are clear. The differences of N, C:N ratio and P analytes values between high centers and depressed low centers, the two features in which a LC may develop, can be explained by the hydrological conditions of these features. For N and C:N, the same process applies as in LCs and Rs explained before, even though the differences between them now are significant.

As for the difference in total phosphorus, it can be explained through its high correlation with iron. In mires, a fraction of P is complexed with organic compounds fixated with Fe. In this study, the high correlation indicates that a large fraction of organic P forms is associated with Fe. In an oxidizing soil environment such as in dry HCs, the mobility of Fe released by weathering is severely restricted by the insolubility of the hydroxide $Fe(OH)_3$, which has a high Ksp. In contrast, the solubility of $Fe(OH)_2$ is greater, which means that in an anaerobic environment such as in waterlogged DLCs and LCs, the dissolved Fe concentration is higher and the mobility of Fe released by weathering is much less restricted (Chesworth and Macias Vazquez, 1985). As a large fraction of P is associated with Fe, this explains the different values of P found in these features. Although it would be expected a similar behavior in Rs than in HCs (both above the water table), they are in a different stage of the thermokarst polygon cycle, which means that different dynamics may affect them, and that is why in this study few similarities have been found between them, although they are in a similar thawing state (permafrost aggradation).

4.2 Geomorphological approach

The total land cover of themokarst lakes and drained thermokarst lake basins mapped in within the studied area is much lower than found in previous studies, due to the Sagavanirktok river and the high slope on the west side taking half of the space. However, in the FA, results agree with previous mapping efforts of permafrost-affected arctic lowlands. The cover estimates for thermokarst lakes and and DTLBs align closely with previous studies in close and similar regions (Wang et al., 2012; Farqhurson et. al, 2016), but they differ from observations in similar substrates on the northern Seward Peninsula (Jones et al., 2012) and in the Kolyma lowlands (Veremeeva and Gubin, 2009), which DTLBs and thermokarst lakes were much greater. Farqhurson et al. (2016) suggest that this difference may be because most thermokarst lakes on the Seward Peninsula have developed on a flat plain rather than in the foothills. The mean slope for the aeolian silt region of the Arctic Foothills is 0,30º, whilst on the Seward Peninsula lowlands is only 0,15º, which is similar to the areas on the Arctic Coastal Plain. The slope then is steep enough in the studied zone to facilitate the runoff of meltwater from degrading ice-wedge polygons, becoming channelized instead of ponding and forming thermokarst lakes. This would also explain the lack of thermokarst lakes on the west side of the studied area, where the slope is much higher (Annex 3). The same would apply for the mean size, which near the coast increases. In this study, the mean size of thermokarst lakes is much higher than

found by Farqhurson et al. (2016), but that is probably because no smaller than 20 ha lakes were mapped.

Also, the greater DTLBs land cover compared to thermokarst lakes is due to the fact that the basins are formed by multiple generations of coalescent, drained lakes, so they end up covering a wider area than lakes. The same explanation can be applied regarding the higher mean size of DTLBs compared to thermokarst lakes.

Thermokarst lakes sometimes exhibit similar orientation, with their long axes aligned more or less parallel to one another. In some areas, it appears to be related to the direction of the dominant winds that blow across the lakes in summer (Coté and Burn, 2002; Hinkel et al., 2005). However, in some cases the orientation of the primary ice-wedge network during lake formation, uneven distribution of ground ice or preferential retrogressive thaw slum activity on slopes may influence the final shape (Grosse et al, 2013; Séjourné et al., 2015). In the studied area thermokarst lakes and DTLB show no preferential direction, contrary to the ones on the Arctic Coastal Plain to the north, probably due to the wind being weaker than in the coast.

Beaded streams cover around the same area (less than 1%) as mapped in previous studies (Farqhurson et al., 2016). Despite their restricted occurrence, beaded streams play an important role in sediment and nutrient transport through tundra watersheds (Arp et al., 2015).

Changes to thermokarst lakes dynamics due to the warming climate, including enhanced degradation of the surrounding permafrost will likely have fundamental impacts on these systems, with consequences for lakes properties and distribution, landscape and ecosystem character, land cover and greenhouse gas emissions (Grosse et al, 2013).

Finally, the carbon stock by land cover found in this study is consistent with what Michaelson et al. (1996) found in the same area for the first meter (88 kg/m^3), although the mean for the northern foothills (the regional area) was lower (44 kg/m^3). When comparing with other previous literature the results have been found to be also much higher than in previous literature: 3,9 (Oechel and Billings 1992) and 4,5 (Post et al., 1982). This big difference is due to the samples being extracted from the same basin, which has a higher carbon stock than others in the same regional area (Michaelson et al., 1996).

The higher stock found in this study highlights the importance to preserve this area as a carbon storage. Permafrost thaw is seen as one of the most important "tipping elements" that could precipitate a runaway greenhouse effect. To avoid such a destructive scenario, it is critical that the world's permafrost and its peatlands stay frozen and retain their carbon deposits (Kolodziejczyk, B. et al., 2019). Conserving, restoring and improving the management of organic soils and undrained peatlands can substantially contribute to reducing atmospheric greenhouse gas (GHG) concentrations and provide other vital environmental services (Joosten, H. et al., 2012).

5 Conclusions

Depth significantly affected the concentrations of most studied analytes, some of which were not significantly different between features, which indicates that OM deposition and accumulation, rivers detrital input, groundwater circulation and freeze-thaw seasonal processes may be controlling variations with depth compared to microtopography.

Comparisons amongst microtopographic features have shown significant differences, particularly between the most extreme PF

degrading and non-degrading features (DLCs vs HCs). In more degraded features, lower C/N values happens due to its vegetation and nitrogen accumulation; and reduced conditions results in calcium and phosphorus (organic forms associated to iron) being lower, while in non-degraded features the opposite happens. This means thermokarst processes produce landscape and relief changes in polygonal mires, favoring peat and lithogenic elements accumulation and in some areas and oxidation and decay in others. Due to these changes in the physicochemical conditions of the ground soil, the ecosystem functioning is altered.

Given the importance of microtopography and depth variations, additional studies are suggested to better understand spatial controls on active layer physiochemistry in a broader Arctic context.

On a coarser scale, big thermokarst landforms cover a wide area, in which DTLBs and thermokarst lakes are the dominant features. Warmer temperatures may cause the expansion of these features, although in the Foothills area, due to its steep slope, over the long term it might favor drainage and reduce their cover.

Finally, the high total carbon stock measured in this study highlights the importance of these soils as carbon storages and, given the physicochemical changes because of ice thaw, their susceptibility to being altered and emit GHGs.

More research on primary geomorphic and biochemical processes needs to be carried out to fully understand the global carbon cycle, atmospheric GHGs concentrations, surface energy balance and the impacts of global climate change on these environments.

6 References

Arp, C. D., Whitman, M. S., Jones, B. M., Grosse, G., Gaglioti, B. V., & Heim, K. C. (2015). Distribution and biophysical processes of beaded streams in Arctic permafrost landscapes. *Biogeosciences*, 12(1), 29-47.

Monitoring, A. (2017). Snow, Water, Ice and Permafrost in the Arctic (SWIPA); Summary for Policy-makers.

Ballantyne, C. K. (2018). *Periglacial geomorphology*. John Wiley & Sons.

Biasi, C., Wanek, W., Rusalimova, O., Kaiser, C., Meyer, H., Barsukov, P., & Richter, A. (2005) Microtopography and Plant-Cover Controls on Nitrogen Dynamics in Hummock Tundra Ecosystems in Siberia. *Arctic, Antarctic, and Alpine Research, 37*(4), 435-443.

Biester, H., Hermanns, Y. M., & Cortizas, A. M. (2012). The influence of organic matter decay on the distribution of major and trace elements in ombrotrophic mires–a case study from the Harz Mountains. *Geochimica et Cosmochimica Acta, 84*, 126-136.

Brown, R.J.E. (1960). The distribution of permafrost and its relation to air temperature in Canada and the USSR. *Arctic 13*(3), 163-177.

Chesworth, W. and Macias Vasquez, F., (1985). pe, pH, and podzolization. *Am. J. Sci. 285*, 128–146.

Cortizas, A. M., Biester, H., Mighall, T., & Bindler, R. (2007). Climate-driven enrichment of pollutants in peatlands.

Côté, M. M., & Burn, C. R. (2002). The oriented lakes of Tuktoyaktuk Peninsula, western Arctic coast, Canada: A GIS-based analysis. *Permafrost and Periglacial Processes, 13*(1), 61-70.

Farquharson, L. M., Mann, D. H., Grosse, G., Jones, B. M., & Romanovsky, V. E. (2016). Spatial distribution of thermokarst terrain in Arctic Alaska. *Geomorphology*, *273*, 116-133.

Frohn, R. C., Hinkel, K. M., & Eisner, W. R. (2005). Satellite remote sensing classification of thaw lakes and drained thaw lake basins on the North Slope of Alaska. *Remote sensing of environment*, 97(1), 116-126.

Giblin, A. E., Nadelhoffer, K. J., Shaver, G. R., Laundre, J. A., & McKerrow, A. J. (1991). Biogeochemical diversity along a riverside

toposequence in arctic Alaska. *Ecological monographs*, *61*(4), 415-435.

Grosse, G., Jones, B. M., & Arp, C. D. (2013). Thermokarst lakes, drainage, and drained basins.

Hinkel, K. M., Frohn, R. C., Nelson, F. E., Eisner, W. R., & Beck, R. A. (2005). Morphometric and spatial analysis of thaw lakes and drained thaw lake basins in the western Arctic Coastal Plain, Alaska. *Permafrost and Periglacial Processes*, *16*(4), 327-341.

Hugelius, G., Tarnocai, C., Broll, G., Canadell, J.G., Kuhry, P., & Swanson, D.K. (2013). The northern circumpolar soil carbon database: Spatially distributed datasets of soil cover and soil carbon storage in the northern permafrost regions. *Earth System Science Data*, *5*(1), 3–13. https://doi.org/10.5194/essd-5-3-2013

Hugelius, G., Strauss, J., Zubrzycki, S., Harden, J.W., Schuur, E.A.G., Ping, C.L. et al. (2014). Estimated stocks of circumpolar permafrost carbon with quantified uncertainty ranges and identified data gaps. *Biogeosciences*, *11*(23), 6573–6593. https://doi.org/10.5194/bg-11-6573-2014

Ivanov, K.E. (1948). Filtration in the top layer of convex mire massifs. *Meteorology and Hydrology*, *2*, 46–59.

Jones, M. C., G. Grosse, B. M. Jones, and K. Walter Anthony (2012). Peat accumulation in drained thermokarst lake basins in continuous, ice-rich permafrost, northern Seward Peninsula, Alaska. *Journal of Geophysical Research: Biogeoscience*, *117*(G2). https://doi.org/10.1029/2011JG001766

Joosten, H., Tapio-Biström, M. L., & Tol, S. (2012). *Peatlands: guidance for climate change mitigation through conservation, rehabilitation, and sustainable use*. Rome: Food and Agriculture Organization of the United Nations.

Jorgenson, M. T., & Shur, Y. L. (2007). Evolution of lakes and basins in northern Alaska and discussion of the thaw lake cycle. *Journal of Geophysical Research: Earth Surface*, *112*(F2).

Jorgenson, M. T., Shur, Y.L. and Osterkamp, T.E. (2008). Thermokarst in Alaska. Proceedings of the Ninth International Conference on Permafrost 1, 869-876. *Fairbanks, AK: University of Alaska Fairbanks*.

Kaufman, D. S., & Hopkins, D. M. (1986). Glacial history of the Seward Peninsula.

Kolodziejczyk, B., Kofler, N., Araya, M., Bull, J., Champer, J., Liu, C. & Garcia, L. C. (2019). Frontiers 2018/19: Emerging Issues of Environmental Concern.

Kuhry, P., Vitt, D. H., 1996. Fossil carbon/nitrogen as a measure of peat decomposition. *Ecology*, *77*(1), 1996, 271-275.

Lacelle, D., A. Doucet, I. D. Clark, and B. Lauriol (2007). Acid drainage generation and seasonal recycling in disturbed permafrost near Eagle Plains, Northern Yukon Territory, Canada. *Chemical geology*, *243(*1), 157–177.

Martini, I. P., Cortizas, A. M., & Chesworth, W. (2007). *Peatlands: evolution and records of environmental and climate changes*. Elsevier.

Michaelson, G. J., Ping, C. L., & Kimble, J. M. (1996). Carbon storage and distribution in tundra soils of Arctic Alaska, USA. *Arctic and Alpine Research*, *28*(4), 414-424.

Parish, F., Sirin, A., Charman, D., Joosten, H., Minaeva, T. & Silvius (2008). Assessment on peatlands, biodiversity and climate change. *Kuala Lumpur, Global Environment Centre and Wageningen, Wetlands International*, 179.

Oechel, W. C., & Billings, W. D. (1992). Effects of global change on the carbon balance of arctic plants and ecosystems. *Arctic ecosystems in a changing climate: an ecophysiological perspective*, 139-168.

Pestryakova, L. A., Herzschuh, U., Wetterich, S., & Ulrich, M. (2012). Present-day variability and Holocene dynamics of permafrost-affected lakes in central Yakutia (Eastern Siberia) inferred from diatom records. *Quaternary Science Reviews*, *51*, 56-70.

Post, W. M., Emanuel, W. R., Zinke, P. J., & Stangenberger, A. G. (1982). Soil carbon pools and world life zones. *Nature*, *298*(5870), 156-159.

Schuur, E. A., Vogel, J. G., Grummer, K. G., Lee, H., Sickman, J. O., & Osterkamp, T. E. (2009). The effect of permafrost thaw on old carbon release and net carbon exchange from tundra. *Nature*, *459*(7246), 556–559. https://doi.org/10.1038/nature08031

Séjourné, A., Costard, F., Fedorov, A., Gargani, J., Skorve, J., Massé, M., & Mège, D. (2015). Evolution of the banks of thermokarst lakes in Central Yakutia (Central Siberia) due to retrogressive thaw slump activity controlled by insolation. *Geomorphology*, *241*, 31-40.

Veremeeva, A., & Gubin, S. (2009). Modern tundra landscapes of the Kolyma Lowland and their evolution in the Holocene. *Permafrost and periglacial processes*, *20*(4), 399-406.

Walter, K. M., J. P. Chanton, F. S. Chapin III, E. A. G. Schuur, and S. A. Zimov (2008). Methane production and bubble emissions from arctic lakes: Isotopic implications for source pathways and ages, Journal of Geophysical Research: Biogeosciences, 113 (G3). https://doi.org/10.1029/2007JG000569

Wang, J., Shen, Y., Hinkel, K.M., Lyons, E.A. (2012. Drained thaw lake basin recovery on the western Arctic Coastal Plain of Alaska using high resolution digital elevation models and remote sensing imagery. *Remote Sensing Environment, 119*, 325–336.

Wilson, F. H., Hults, C. P., Mull, C. G., & Karl, S. M. (2015). *Geologic map of Alaska*. US Department of the Interior, US Geological Survey.

Zhang, T., Barry, R. G., Knowles, K., Heginbottom, J. A., & Brown, J. (2008). Statistics and characteristics of permafrost and ground-ice distribution in the Northern Hemisphere. *Polar Geography*, *31*(1-2), 47–68. https://doi.org/10.1080/10889370802175895

7 Annexes

Annex 1: Field scenes of the studied features

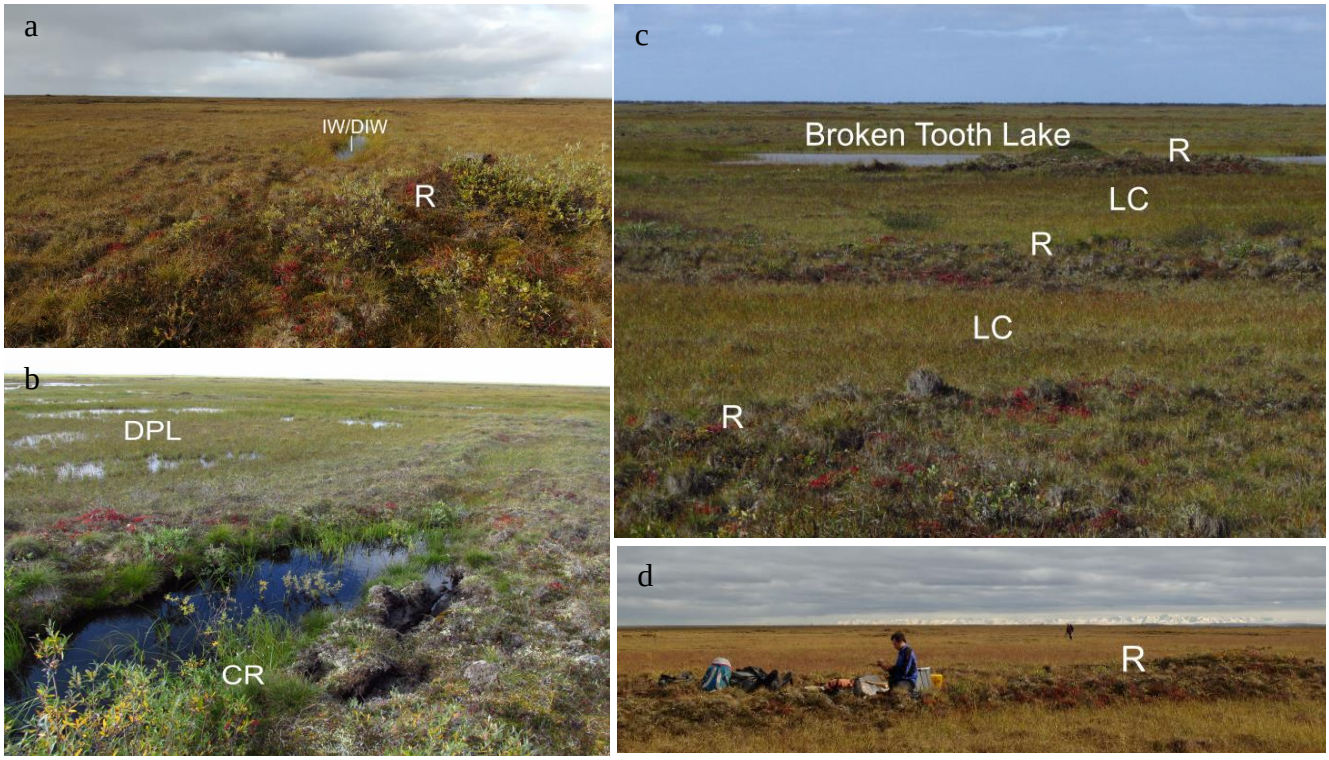

Fig. 18. a) Rim that is flooded on the background, above the ice wedge (it might be degraded if thaw has started). It is not yet a collapsed rim. b) Rim that has collapsed and a depressed low center (water level is almost completely above the vegetation cover). The vegetation on the CR is clearly differentiated from the surrounding vegetation (former rim). c) Sequence of rims and low centers with the Broken Tooth Lake on the background. d) Rim clearly differentiated from the surrounding vegetation (low centers).

Annex 1: Landsat 8 scene of the studied area with b.c. 6-5-2

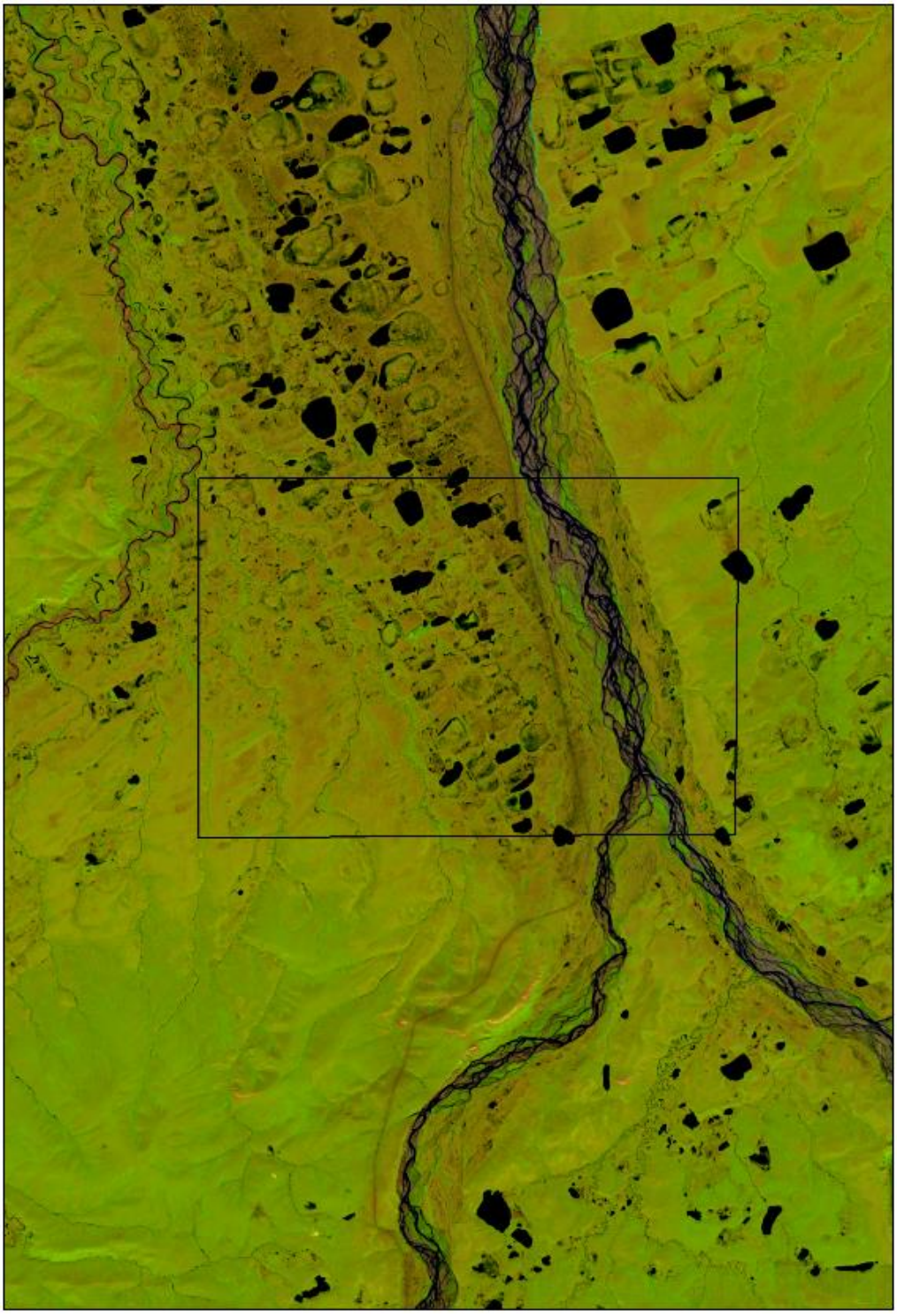

Fig. 19. Landsat 8 OLI/TIRS scene from 8 July 2019 (path 74, row 11) with the band combination 6-5-2 set (6 – SWIR 1; 5 – near infrared; 2 – blue).

Annex 2: Cartography of Northern Alaska

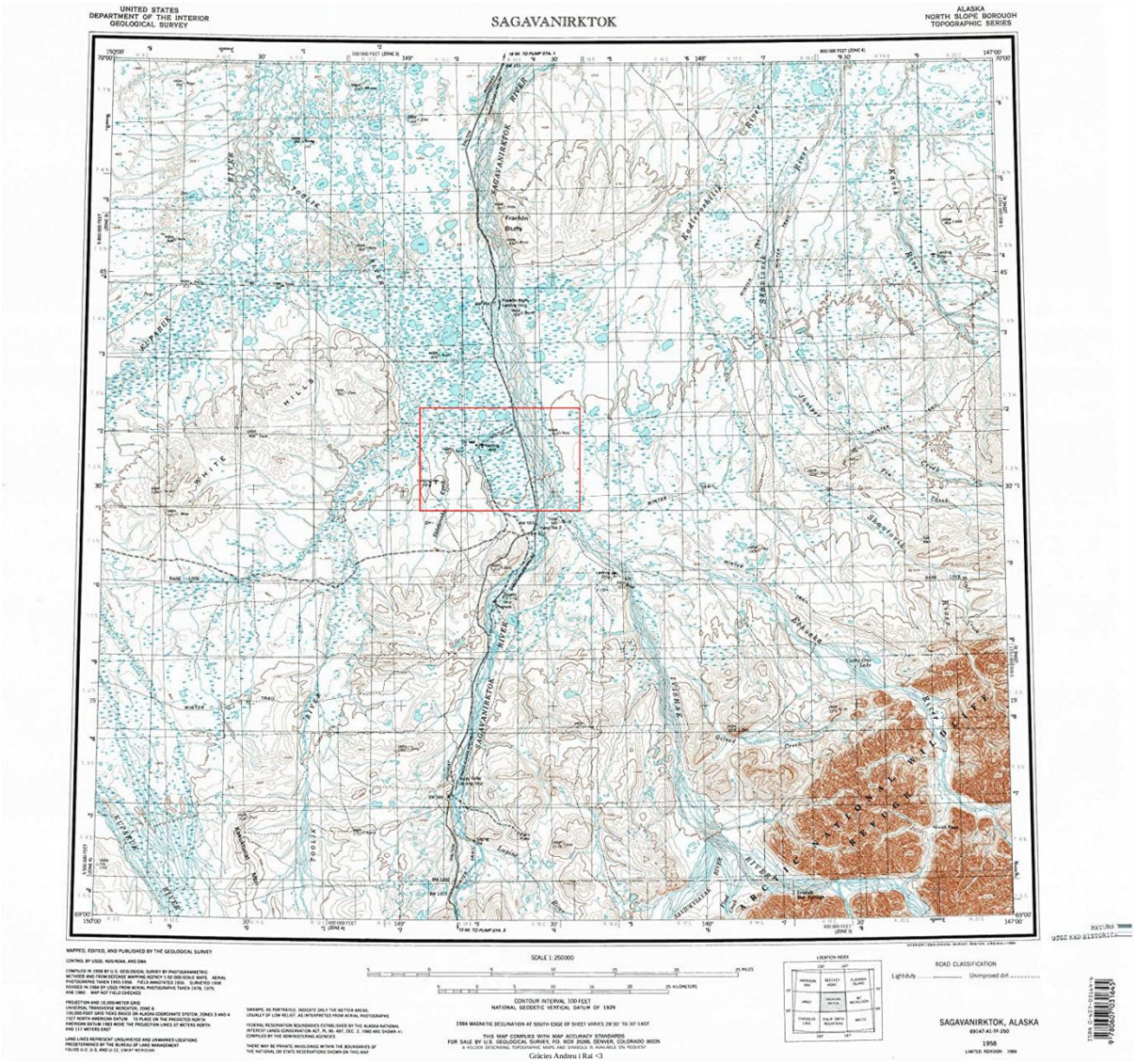

Fig. 20. Cartography of Northern Alaska. Studied area located in the red square.